Research Article

Riyad A. Almaimani*

Synthesis and characterization of Pluronic F-127-coated titanium dioxide nanoparticles synthesized from extracts of *Atractylodes macrocephala* leaf for antioxidant, antimicrobial, and anticancer properties

https://doi.org/10.1515/gps-2023-0100 received June 15, 2023; accepted September 4, 2023

Abstract: Globally, nanotechnology is generating significant interest because of its promise in a wide range of industries. The most commonly used nanoparticles are titanium dioxide nanoparticles (PF-127 coated TiO2 NPs), which can be formulated with physical, chemical, and environmental factors. The establishment of an economical and environmentally beneficial method for its fabrication is due to increasing concerns about human health impacts. In this exploration, green Pluronic F-127 (PF-127) coated TiO2 NPs using leaf extracts of Atractylodes macrocephala have been formulated and studied through various methods. PF-127 coated TiO2 NPs were 60 nm large and a polygonal rutile-type crystalline structure was observed. Moreover, the NPs' antimicrobial capacity against several pathogens was investigated. The cytotoxicity of the NPs against HEp-2, KB, and Vero cell lines was assessed using the MTT test. Increased antimicrobial potential of PF-127 coated TiO2 NPs against several pathogens was noted. Furthermore, NPs displayed remarkable antioxidant activity, which increased with concentration. The NPs exhibited significant cytotoxic effects against HEp-2 and KB cell lines but failed to demonstrate toxicity against Vero cells. This is indicative of their cytotoxic potential against cancer cell lines and non-toxic nature towards healthy cells. This indicates that PF-127 coated TiO₂ NPs possess beneficial antimicrobial and antitumor properties.

1 Introduction

Nanotechnology is a fascinating technological advancement focused on developing materials with superior properties and innovative capabilities. The utilization, as well as applicability of nanoparticles (NPs), are particularly prevalent in the fields of chemicals, medicine, healthcare, automobiles, cosmetics, and energy [1]. In comparison to the starting materials, the produced NPs typically have a high surface-to-volume ratio [2].

Noble metal NPs have attracted the most popularity among inorganic NPs owing to their unique properties. These properties enable major implementation in several disciplines like photonics, microelectronics, medicine, and catalysis [3]. Titanium nanoparticles (Pluronic F-127 coated TiO2 NPs), particularly, are regarded as desirable nanomaterials due to their simplicity of management, low cost, excellent resistance to chemical erosion, nontoxicity, excellent stability, and antimicrobial and photocatalytic activities [4–6]. It is an N-type semiconductor and is utilized in a plethora of applications like wastewater treatment, dyesensitized solar cells, photoionized circuits, and lithiumion batteries [7].

Pluronic F-127 (PF-127) coated TiO2 NPs are typically formulated by sol–gel, chemical vapor deposition, hydrothermal, and chemical precipitation processes. However, these processes have drawbacks because of high energy, pressure, temperature, and harmful chemicals [8,9]. Hence, environmentally friendly and inexpensive synthesis approaches for PF-127 coated TiO2 NPs are required

Keywords: Pluronic F-127, titanium dioxide nanoparticles, *Atractylodes macrocephala* leaf extract, HEp-2 cancer cells, KB cell line, Vero cell line

^{*} Corresponding author: Riyad A. Almaimani, Department of Biochemistry, Faculty of Medicine, Umm Al-Qura University, Makkah, Saudi Arabia, e-mail: ramaimani@uqu.edu.sa

to make them appropriate for large-scale production. The utilization of naturally derived products as environmentally friendly reducing agents to produce metal oxide NPs is a result of the rising focus on green chemistry [10]. In order to synthesize stable, appropriate-sized, and soluble NPs with minimal energy usage, green synthesis strategies are required [11].

Green synthesis techniques utilizing biological preparations as reducing agents allow us to synthesize PF-127 coated TiO2 NPs at a low cost and with no environmental impact. In the past, a variety of fungi, bacteria, microorganisms, and plant extracts were utilized to fabricate NPs [12]. Plants offer excellent availability, biocompatibility, and biodegradability among these life forms [13]. Numerous phytochemicals from plants, including alkaloids, polyphenols, tannins, terpenoids, and alcoholic compounds, are easily obtainable in herbal extracts. They can stabilize and reduce the environmental impact of NP synthesis. Additionally, the metabolites present in plant extracts are essential NP stabilizing or capping agents. Further, some research has indicated that plant extracts can yield relatively more stable metal NPs than those produced by microorganisms and can reduce metal ions more efficiently than bacteria [14].

In the literature, it has been observed that PF-127 coated TiO₂ NPs produced from plant extracts exhibit inhibitory action against a plethora of microbial pathogens [15]. Plant extracts of *Aloe barbadensis* [16], *Trigonella foenum-graecum* [11], *Citrus limon* [17], *Cochlospermum gossypium* [18], *Artemisia haussknechtii* [19], *Eichhornia crassipes* [20], *Echinacea purpurea* [21], *Syzygium cumini* [22], *Carica papaya* [23], and *Citrus sinensis* [24] are now being extensively employed in synthesis techniques to produce green PF-127 coated TiO₂ NPs [19]. However, the leaves from the plant *Atractylodes macrocephala* have not been employed for green PF-127 coated TiO₂ NP synthesis.

The formation of stable structures for effective drug delivery is essential when designing nanodrugs for therapeutic delivery. Therefore, delivery methods have shifted to more regulated and stable systems, including polymeric NPs [25]. Particularly, as these polymers can be combined with both hydrophilic and hydrophobic compounds, attention has recently increased on polymeric amphiphiles as core components. Pluronic, an amphiphilic block copolymer, has drawn considerable attention from the drug delivery sector [26].

PF-127 is an amphiphilic copolymer, comprising a central hydrophilic poly-ethylene oxide chain [27]. PF-127 is recognized as an excellent medium for effective drug administration by a variety of parenteral and non-

parenteral routes due to its strong solubilizing properties, low toxicity, and biocompatibility [28]. Over the last decades, extensive research into the functional characteristics of these polymers has led to the creation of several systems widely used as drug delivery mechanisms [29]. An earlier study presented a TiO2@MWCNTs nanocomposite photoanode for photoelectrochemical water splitting, improving the absorption of visible light and electron transfer. The nanocomposite has higher current density under solar irradiation and improved solar-to-hydrogen conversion efficiency [30]. Researchers developed a low-cost method to reduce pristine TiO₂ in 30 min using minimal sodium borohydride, producing colored samples. UV-DRS, X-ray diffraction (XRD), ESR, XPS, field emission scanning electron microscopy (FESEM), and TEM are used as characterization techniques [31].

Previous research explored the green synthesis of copper oxide NPs (CuO NPs) using plant extracts. The review also discusses the cost-effective and environmentally friendly process, revealing aspects of plant physiology and their relationship to NP synthesis, and the multifunctional applications of CuO NPs synthesized with plant extracts in environmental remediation, sensing, catalytic reduction, photocatalysis, biological activities, energy storage, and organic transformations. The previous study also aimed to serve as a guide for readers interested in plant extract-mediated biosynthesis of CuO NPs and their potential applications [32]. Chromic oxide NPs (Cr₂O₃ NPs) are a significant inorganic NP with numerous applications in various fields. Despite their ecological and economic challenges, biological methods using plant materials have shown potential for their synthesis. These NPs have numerous health, environmental, economic, and medicinal benefits, including antibacterial, antifungal, antioxidant, anticancer, antileishmanial, antiviral, and anti-diabetic properties. However, challenges in clarifying formation reactions remain unresolved. Modern advancements in the synthesis, characterization, and applications of photosynthesized Cr₂O₃ NPs are discussed [33].

In traditional Chinese medicine, *A. macrocephala* Koidz has gained attention because it is an herb from the Compositae family. In China, it has been used for millennia as food and medicine. A variety of compounds have been identified in *A. macrocephala*, such as essential oils, amino acids, sesquiterpenoids, resins, polysaccharides, and other substances [34]. Pharmacological studies and clinical experience indicate that the plant extracts have a wide range of bioactive properties against diarrhea, stomach discomfort, intestines, liver, and kidney disorders [35]. The digestive tract is frequently treated with it, and the gastrointestinal tract is also regulated by it [36]. Lactones

DE GRUYTER

potential as biocompatible and bioactive agents.

We aim to synthesize and characterize TiO2 NPs coated with PF-127 using A. macrocephala leaf extracts for antioxidant, antimicrobial, and anticancer properties. As an ecofriendly and sustainable alternative to chemical reagents, natural extracts may enhance the properties of NPs. The NPs coated with PF-127 provide improved biocompatibility, making them versatile for antimicrobial and anticancer, and displayed remarkable antioxidant activity, which increased with concentration. Synergistic effects may result from combining the NPs with the bioactive compounds contained in A. macrocephala leaf extract. The NPs exhibited significant cytotoxic effects against HEp-2 and KB cell lines but failed to demonstrate toxicity against Vero cells. This indicates their cytotoxic potential against cancer cell lines and non-toxic nature towards healthy cells. Various applications are possible for the NPs due to their comprehensive evaluation, which covers antioxidant, antimicrobial, and anticancer properties. The research aligns with green nanotechnology principles, reducing reliance on traditional chemical methods. Understanding the mechanisms behind NPs' properties could lead to more targeted therapies. Optimizing the coating consistency, NP size, or extract concentration could be included in future optimizations. The interdisciplinary approach encourages collaboration and knowledge exchange among experts in different fields, fostering innovation.

In the present investigation, the biosynthesis of PF-127 coated TiO2 NPs with the leaf extract of A. macrocephala and their biomedical applications such as antioxidant, antimicrobial, and anticancer activities were assessed.

2 Materials and methodology

2.1 Materials

Chemicals such as Titanium isopropoxide (TTIP) and PF-127 were procured from Sigma Aldrich, USA. All the corresponding assay kits to estimate biochemical markers were purchased from Abcam, USA.

2.2 Preparation of A. macrocephala leaf extract

10 g A. macrocephala fresh leaf extract was mixed with 100 ml ethanol and heated for 20 min at 80°C. The suspension was filtered using filter paper, and the resultant extract was stored at 4°C.

2.3 Preparation of PF-127 coated TiO₂ NPs

To prepare PF-127 coated TiO₂ NPs, 0.1 M of TTIP and 0.5 g of PF-127 were added with 100 ml of A. macrocephala extract (pH of solution 8). The green-yellow suspension was stirred continually for 5 h at 80°C. The white precipitate was dried at 120°C for 1 h. The formed PF-127-coated TiO₂ NPs were calcined for 5 h at 800°C.

2.4 Characterization of PF-127 coated TiO₂ NPs

The PF-127-coated TiO2 NPs were studied with an XRD (Bruker-AXS D5005). The test was conducted under Cu-Ka radiation at $\lambda = 0.1541$ nm and scanned at 2θ angle between 20 and 90°. A DLS study was performed to examine the average particle size. The test was conducted utilizing NPs at a 90° scattering angle and 25°C. The appearance of PF-127-coated PF-127 coated TiO2 NPs was observed with FESEM (Hitachi s-4800II) and EDAX was employed to determine the elemental composition. To investigate the NP size, transmission electron microscopy (TEM; Jeol Jem-2010F) was employed. The NPs were spread on a copper grid, and exposed to electronic radiation under vacuum. Additionally, an electron beam was utilized to take images after transmitting them via material. Based on fouriertransform infrared spectroscopy (FTIR) spectroscopy (NicoletiS50), functional groups present in PF-127 coated TiO₂ NPs were analyzed. The infrared (IR) spectrum was taken using the reflectance method. The developed NPs were ground with KBr at a 1:100 ratio. The blend was flattened into a disc to make potassium bromide (KBr) discs and scanned at 400-4,000 cm⁻¹ wavelength. The formed NPs were examined using UV-Visible spectroscopy (Shimadzu UV-2550, made in the USA) to validate the development and observe the surface plasmon resonance. The NPs were examined at 1,200-200 nm and the study was conducted three times. Photoluminescence (PL) study scrutinized the optical properties (Roithner Lasertechnik). The spectra were investigated at 350–550 nm at $\lambda_{\rm exc}$ = 470 nm. Triplicate tests were conducted, and the energy band gap was investigated by plotting the Tauc curve with the equation given below

$$(h\nu\alpha)1/n = A(h\nu - E_g) \tag{1}$$

where h is the Planck's constant; A is a constant proportion; α is the absorption coefficient; ν is the vibration frequency; $E_{\rm g}$ is the band gap; and n is the sample transition nature.

2.5 Antimicrobial activity

The antimicrobial potentials of the PF-127 coated TiO₂ NPs against *S. aureus*, *B. megaterium*, *B. subtilis*, *S. dysenteriae*, *E. coli*, *P. aeruginosa*, and *C. albicans* strain was evaluated by disc diffusion technique. For this investigation, molten nutrient agar medium was utilized. Micropipettes were used to transfer samples at 1, 1.5, and 2 mg·ml⁻¹ dosages along with the positive control onto the bacteria-seeded plates after inoculation. After that, the plates were left for incubation for 24 h. The inhibition zones were noted following the incubation. The positive control against all the tested microorganisms employed was amoxicillin (Hi-Media) [38,39].

2.6 Evaluation of antioxidant activity

DPPH was utilized to evaluate the capacity of PF-127 coated ${\rm TiO_2}$ NPs to quench free radicals with a few minor adjustments. In brief, 500 ml of 0.2 mM DPPH solution (in 50% ethanol) were combined with NPs at varied concentrations (1.25, 2.5, 5, 10, 20, and 40 $\mu {\rm g \cdot ml}^{-1}$). The reaction solution was shaken for 30 min, and absorbance at 517 nm was calculated and compared to a control. Increased antioxidant action is shown by a decrease in DPPH absorption. The equation to estimate the radical scavenging potential is given below

Scavenging effect (%)
=
$$(1 - A_{\text{samples.} 517 \text{ nm}}/A_{\text{control.} 517 \text{ nm}}) \times 100$$
 (2)

2.7 *In vitro* anticancer activity of PF-127 coated TiO₂ NPs

2.7.1 Culture and maintenance of cell lines

HEp-2 (human laryngeal cancer cells), KB (mouth), and Vero cells (normal) were acquired from ATCC, USA, and grown in DMEM medium for 24 h. The cells were collected after reaching 80% confluency and employed in further investigations.

2.7.2 Cytotoxicity assay

The cytotoxicity of PF-127 coated TiO_2 NPs was assessed using MTT assay. Using 24-wellplate, the cells were cultivated for 24 h and following the incubation time, the cells were exposed to the NPs at 2, 4, 8, 16, 32, and $64 \, \mu g \cdot ml^{-1}$ for 24, 48, and 72 h. Afterwards, the cells were added to MTT (5 mg·ml⁻¹) for 3 h. After that, DMSO was mixed to liquefy the formazan sediments before the absorbance was taken at 540 nm. Using the program OriginPro8, the IC50 concentration of the NPs were measured.

2.8 Statistical analysis

All studies were executed in triplicate, and then one-way ANOVA and a post hoc Tukey test were applied to statistically assess the data. Data are given as mean value \pm SD with p < 0.05 as significant.

3 Results

3.1 Spectral characterization of PF-127 coated TiO₂ NPs

UV-Vis spectroscopy is the procedure that is employed most frequently to characterize the structural properties of NPs.

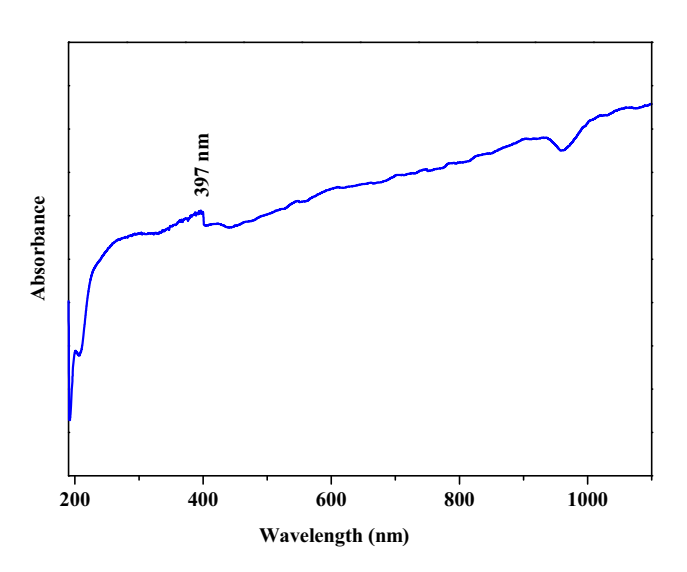


Figure 1: UV-Vis spectrophotometer analysis of synthesized of PF-127 coated TiO_2 NPs.

The absorption spectra of green PF-127 coated ${\rm TiO_2}$ NPs annealed at 600°C is depicted in Figure 1. The NP absorption was estimated in the range between 200 and 1,100 nm and the PF-127 coated ${\rm TiO_2}$ NP in its rutile phase form exhibits an optical absorption range of around 397 nm.

The FTIR spectra of green synthesized PF-127 coated TiO₂ NPs is illustrated in Figure 2. Peaks corresponding to O–H stretching and bending was noticed at 3,427 and 1,639 cm⁻¹, respectively. The typical peaks were noticed at 2,924 cm⁻¹ for asymmetric stretching, 2,854 cm⁻¹ for symmetric stretching, and 1,384 cm⁻¹ for an O–H bending [40]. The strong band below 1,050 cm⁻¹ corresponds to Ti–O stretching vibrations. The O–Ti–O stretching band was located at 779, 548, and 478 cm⁻¹ [41].

Figure 3 demonstrates the PL spectrum of PF-127 coated ${\rm TiO_2}$ NPs with an excitation wavelength of 325 nm. For PF-127 coated ${\rm TiO_2}$ NPs, PL emission was noted at 430, 438, 484, 513, and 527 nm. The blue emission bands at 430, 438, and 484 nm are attributed to singly ionized tin vacancies. The green emission indicates that the oxygen vacancy (Ov) band is located between 513 and 527 nm [42].

3.2 Morphology and chemical elements of green synthesized PF-127 coated TiO₂ NPs

Surface morphological characteristics of green PF-127 coated ${\rm TiO_2}$ NPs were observed using FESEM/TEM/SAED patterns, as revealed in Figures 4 and 5. The polygonal structure of PF-127 coated ${\rm TiO_2}$ NPs is noticeable in FESEM

(Figure 5a) and TEM (Figure 4a–c) images. The size of 54 nm, as exhibited by XRD, is consistent with the findings.

The SAED pattern authorizes the PF-127 coated ${\rm TiO_2}$ rutile crystalline phase generation (Figure 4d). EDAX analysis, with elemental mapping and spectrum analysis, can verify NP composition and distribution patterns. Each element has a peak in an X-ray area that corresponds to its energy level [43]. The chemical constitution of the green PF-127 coated ${\rm TiO_2}$ NPs was determined by an EDAX spectrum, as depicted in Figure 5b. In the PF-127 coated ${\rm TiO_2}$ NPs, copper (Cu), titanium (Ti), and iron (Fe) were the predominant atomic percentages. During the TEM analysis, copper elements might be present due to the copper grid.

3.3 XRD study

An XRD study was conducted to determine the crystallinity of the PF-127 coated ${\rm TiO_2}$ NPs, as depicted in Figure 6a. The crystal structure of the produced PF-127 coated ${\rm TiO_2}$ NPs was discovered to be in the rutile phase based on the XRD pattern (JCPDS Card No. 21-1272) [44]. The diffraction peaks of PF-127 coated ${\rm TiO_2}$ NPs in the rutile phase of 2θ angle at 27.18°, 35.81°, 38.92°, 40.99°, 43.81°, 54.07°, 56.41°, 62.51°, 63.80°, 68.73°, and 69.53°, with diffraction plans (110), (101), (200), (111), (210), (211), (220), (002), (310), (301), and (112), respectively. The crystallinity of the NPs is determined by Debye–Scherrer's equation [45].

Crystallite size
$$(D) = \frac{0.9\lambda}{\beta \cos \theta}$$
 (3)

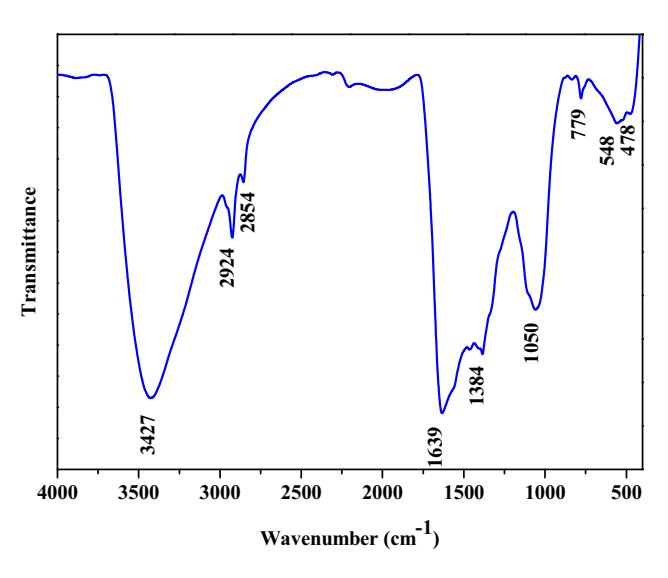


Figure 2: FTIR transmittance vs wavenumber chart of PF-127 coated TiO_2 NPs derived from IR analysis.

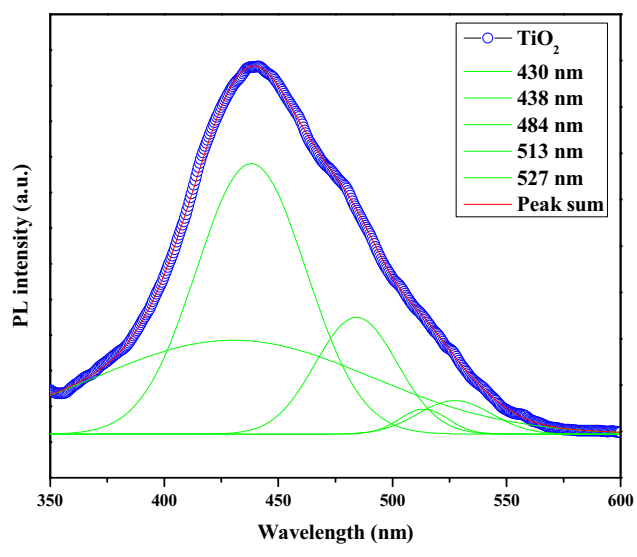


Figure 3: PL spectrum of PF-127 coated TiO₂ NPs.

6 — Riyad A. Almaimani DE GRUYTER

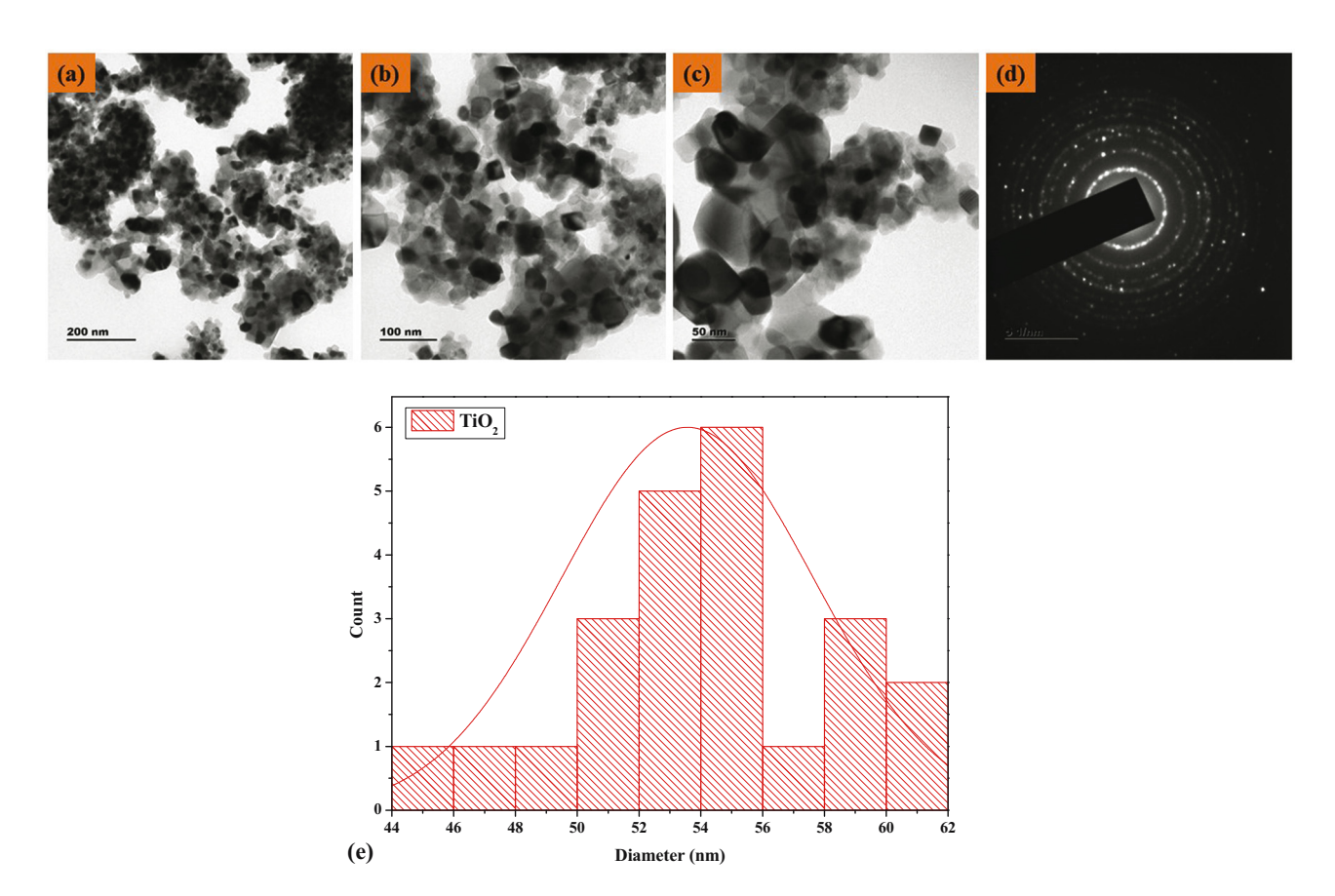


Figure 4: (a–c) TEM images and (d) SEAD pattern of green synthesized PF-127 coated TiO₂ NPs: Lower and Higher magnification TEM image. (e) Histogram of PF-127 coated TiO₂ NPs.

where λ is the X-ray wavelength (1.54060 Å), θ is the Bragg's diffraction angle, and β is the angular peak width at half maximum (radians). After successful synthesis, the particle size of the PF-127 coated TiO₂ NPs has been primarily scrutinized using Debye–Scherrer's equation in addition to analyzing the crystallinity of the material. The Scherrer's equation, which combines the 2θ and full width at half maximum level from XRD finding, is regarded to be the most essential and often employed equation to measure particle size [46].

The size of the PF-127 coated TiO_2 NPs is 60 nm. The hydrodynamic diameter of PF-127 coated TiO_2 NPs was assessed using DLS to obtain particle size information (Figure 6b). The PF-127 coated TiO_2 NPs size was observed at 164 nm because an aqueous medium surrounded the PF-127 coated TiO_2 NPs. This is known as hydrodynamic size. The stability of the NPs was assessed based on their zeta potential, as illustrated in Figure 3b. The results revealed a significant negative zeta potential value of -16.7 mV, indicating a robust colloidal nature of the particles. This observation suggests that the particles exhibited good stability and maintained their colloidal state effectively.

3.4 Green PF-127 coated TiO₂ NPs induce antimicrobial activity

The antimicrobial property of the green synthesized PF-127 coated TiO₂ NPs was assessed against *S. aureus, B. megaterium, B. subtilis, E. coli, S. dysenteriae, P. aeruginosa*, and *C. albicans* pathogens at various sample concentrations (1, 1.5, and 2 mg·ml⁻¹). The inhibition zones of PF-127 coated TiO₂ NPs and conventional antibiotics like amoxicillin against bacterial and fungal strains are depicted in Figure 7a and b. The results revealed that for all of the pathogens examined, increase in the PF-127 coated TiO₂ NPs concentration enhanced the diameters of the inhibitory zones.

This study demonstrates that the green-synthesized PF-127 coated TiO₂ NPs have potential as antimicrobial agents against a range of bacterial and fungal pathogens. The results also suggest that increasing the concentration of these NPs can enhance their antimicrobial efficacy. The study's findings may contribute to the development of new antimicrobial materials or treatments. For most pathogens, as the concentration of PF-127 coated TiO₂ NPs increases,

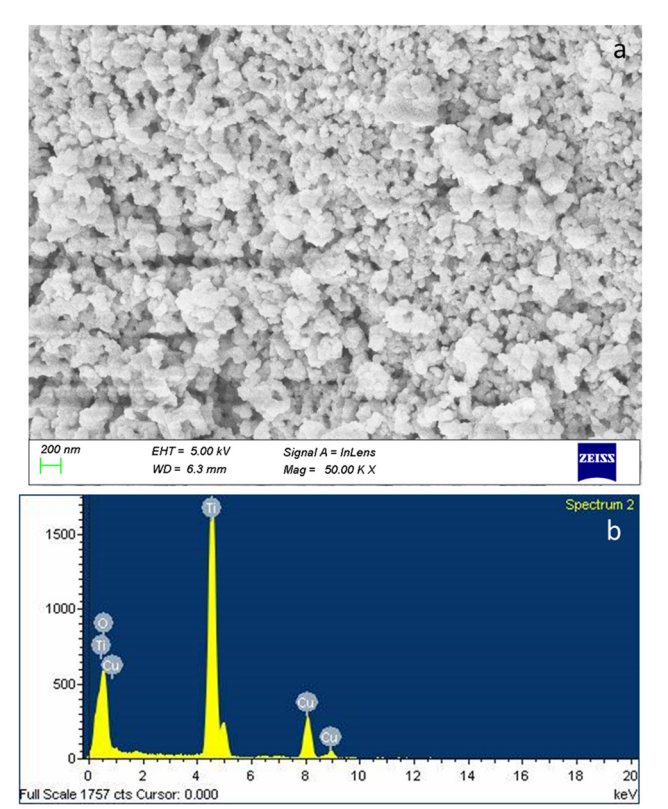


Figure 5: FESEM image of PF-127 coated TiO₂ NPs (a). Elements, weight%, and atomic% of the composition obtained by EDX (b).

the inhibition zone diameter tends to increase. This suggests that higher NP concentrations have a stronger inhibitory effect against these pathogens. In some cases, the inhibition zone diameter for the highest concentration of PF-127 coated TiO_2 NPs $(2\,mg\cdot ml^{-1})$ is greater than that of

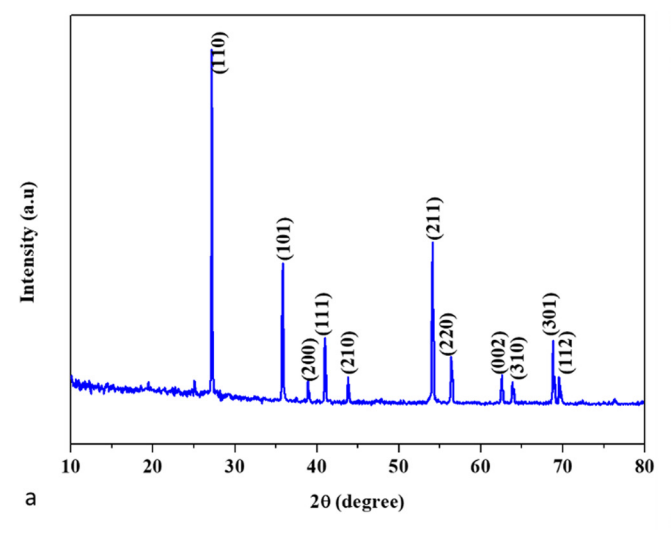
amoxicillin, indicating that the NPs might be more effective against those particular pathogens. The effectiveness of the NPs can vary depending on the pathogen. Some pathogens show higher susceptibility to the NPs at lower concentrations, while others might require higher concentrations for effective inhibition. The presented data suggest that the green-synthesized PF-127 coated TiO₂ NPs have potential as antimicrobial agents, and their effectiveness varies based on the concentration and the target pathogen (Figure 7a and b).

3.5 Green PF-127 coated TiO₂ NPs exhibits antioxidant activity

The antioxidant potential of the PF-127 coated PF-127 coated ${\rm TiO_2}$ NPs was evaluated by examining the potential of the NPs to quench the stable DPPH radical into nonradical state. A high free radical scavenging potential was observed upon treatment with the biosynthesized PF-127 coated ${\rm TiO_2}$ NPs. Moreover, the activity was found to increase the antioxidant activity in a concentration-dependent fashion, with the highest concentration sample exhibiting an inhibition percentage of 75% (Figure 8).

3.6 PF-127 coated TiO₂ NPs induce cytotoxicity against HEp-2 and KB cell lines

The biosynthesized PF-127 coated TiO₂ NPs was scrutinized for their cytotoxicity against HEp-2 (human laryngeal



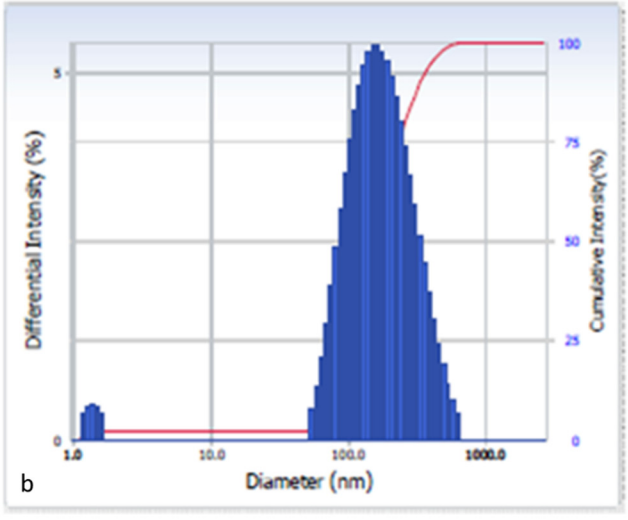


Figure 6: An XRD and DLS pattern of TiO₂ NP coated with PF-127 is shown in (a) and (b).

8 — Riyad A. Almaimani DE GRUYTER

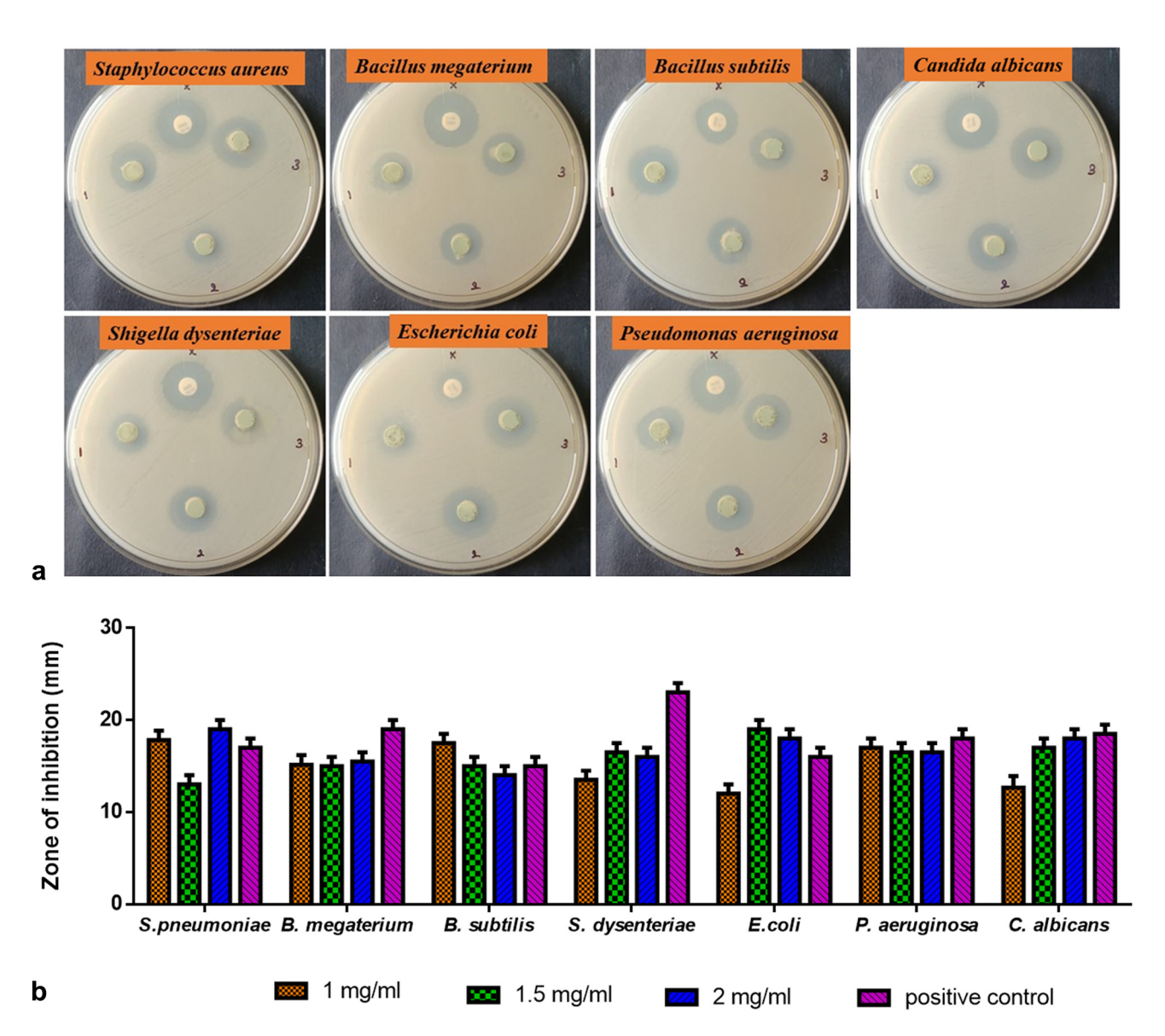
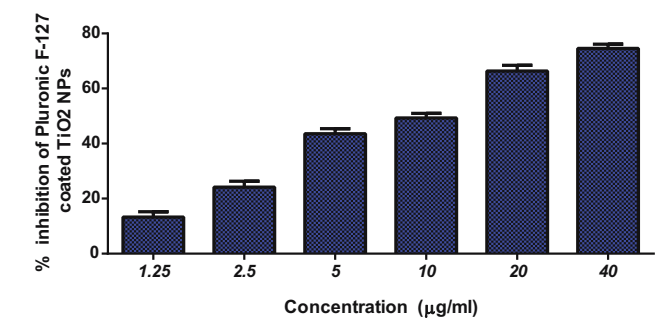


Figure 7: Antibacterial activity of PF-127 coated TiO₂ NPs. NPs inhibit the growth of bacteria (a). Antibacterial activity was determined for PF-127 coated TiO₂ NPs by measuring zone of inhibition (b).

cancer cell line), KB (human epithelial carcinoma cells), and Vero cell lines (Monkey kidney epithelial cell lines) at diverse dosages (2, 4, 8, 16, 32, $64 \,\mu g \cdot ml^{-1}$) at 24, 48, and 72 h. The NPs exhibited significant cytotoxic effects against HEp-2 and KB cells with an IC50 level of 37.9 and 42.2 $\mu g \cdot ml^{-1}$ at 24 h; 30.09 and 18.64 $\mu g \cdot ml^{-1}$ at 48 h; and 16.72 and 11.79 $\mu g \cdot ml^{-1}$ at 72 h, respectively (Figure 9).



4 Discussion

As a metal oxide semiconductor, PF-127 coated ${\rm TiO_2}$ NP in its rutile phase form exhibits an optical absorption range

Figure 8: Antioxidant activity and percentage of inhibition of DPPH free radical by synthesized PF-127 coated TiO_2 NPs. Values are presented as mean value \pm SD (n = 3). Statistical analysis was performed by Student's t-test. **p < 0.01; ***p < 0.001.

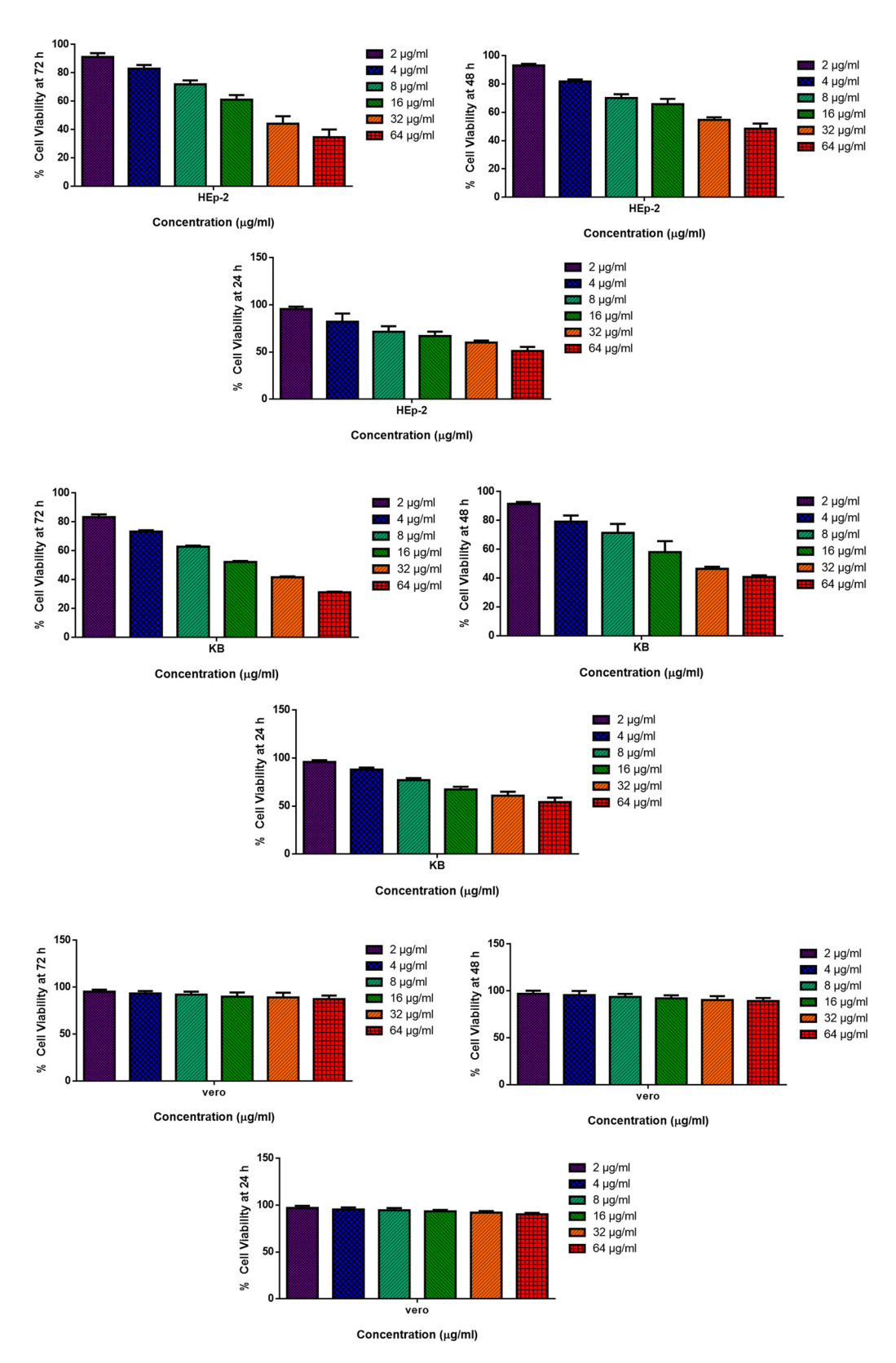


Figure 9: PF-127 coated TiO_2 NPs cause cytotoxicity in HEp-2 (laryngeal cancer cells), KB (mouth), and vero cells (normal). HEp-2, KB, and Vero cells were treated with different concentrations (2–64 μ g·ml⁻¹) of PF-127 coated TiO_2 NPs for 24, 48, and 72 h. The cells were subjected to MTT assay and the values were depicted as mean value \pm SD of three individual experiments.

of around 397 nm [37,47]. The outcomes of the current investigation are in concordance with those of other investigations that reported the synthesis of PF-127 coated TiO₂ NPs using Trigonella foenum and Vitex negundo extracts, where the presence of TiO₂ bands were observed at 400 and 380-400 nm, respectively [11,48]. By analyzing the chemical composition, FTIR could be utilized to assess a variety of materials in bulk and nano forms. The FTIR study revealed information on the biological molecules on the NP surface [3]. It is evident from the FTIR spectroscopic study that A. macrocephala plant extract contains the phytochemicals necessary to reduce the Ti ions in the precursor that is a necessary step in the PF-127 coated TiO₂ NPs. The results are consistent with those obtained from PF-127 coated TiO₂ NP production using extracts from T. portulacastrum and C. quinoa [7]. PL spectroscopic study revealed that the PF-127 coated TiO2 NPs were related to band defects or transitions or to exciton recombination [49].

Techniques including SEM and TEM were extensively utilized to investigate the morphological characteristics of the NPs. These techniques can also be used to establish the size of NPs that have been obtained [50]. The form and surface of the PF-127 coated TiO₂ NPs produced by *A. macrocephala* were different. This might be because *A. macrocephala* leaf extracts contain phytochemicals including terpenoids, polyphenols, steroids, flavonoids, antioxidants, alkaloids, and tannins, whereas chemically produced NPs are typically spherical shaped, arranged in clusters with a relatively larger diameter, and porous in nature [7].

NP build-up on the microbial surface also serves a function in this mechanism by causing the destruction of the cell envelope and the release of intracellular components. The area of interaction between NPs and pathogenic bacteria increases as a result of their enhanced surface area, making them appropriate as antimicrobial agents [51]. The generation of Ti²⁺ ions and their electrostatic interaction with the bacterial cell wall might contribute to the antibacterial action of the NPs. Reactive oxygen species (ROS) are generated due to this interaction that can damage proteins and DNA. This leads to the death of microbes [52,53]. Since Ti NPs contain hydroxyl groups, they can dissolve bacterial outer membranes, causing the bacterium to die [54].

PF-127 coated TiO₂ NPs have displayed remarkable antibacterial activity against several pathogens [55]. Additionally, PF-127 coated TiO₂ NPs produced with fenugreek displayed effective antimicrobial potential and green PF-127 coated TiO₂ NPs synthesized with lemon also exhibited antibacterial activity against *Dickeya dadantii* [11,14]. These outcomes aligned with the prior study since PF-127 coated

TiO₂ NPs synthesized from Kniphofia foliosa root extract exhibited antibacterial effects against *E. coli*, *S. pyogenes*, *K. pneumonia*, and *S. aureus* [56].

Free radicals are generated by external substances or by regular metabolic processes in the body. They can immediately begin the peroxidation of membrane lipids, which results in the excessive accumulation of lipid peroxide [57]. The electron density transfer from the one positioned at O_2 to the electron present at nitrogen in DPPH, leading to a reduced intensity of $n \to \pi^*$ transitions, majorly contributes to the antioxidant effectiveness of the SnO_2 NPs [58]. A similar significant dose-dependent antioxidant activity by green PF-127 coated TiO_2 NPs synthesized with the leaves extract of *Malva parviflora* and *Artemisia haussknechtii* have been documented in various investigations [3,59].

Cancer causes high fatalities in developing countries. It was demonstrated that oxidative stress serves immensely in the initiation and progression of numerous illnesses that affect vital organs, particularly cancer [60]. The therapeutic index of current chemotherapeutic agents is extremely confined, they have poor solubility, and they are toxic to normal tissues [61]. Based on this theory, polymer-based drug delivery devices can ensure highly localized chemotherapeutic drug level in tumor site with minimal negative effects on normal cells [62].

Furthermore, the cell growth was noticed to reduce with higher NP dose. Nonetheless, the NPs did not reveal cytotoxicity to the Vero cells, which demonstrate their nontoxicity nature to non-malignant cells. Higher ROS levels cause oxidative stress inside the cells, which ultimately causes programmed cell death. Additionally, elevated ROS levels have been linked to cell death via damaging mitochondrial membranes [63]. As per the earlier investigations, green-synthesized SnO₂ NPs have revealed considerable antitumor properties [64–66]. To improve the stability of NPs in an aqueous condition, PF127 were employed for encapsulation [67]. It was highlighted that PF-127 can sensitize tumor cells to several drugs [10].

The orange peel extract-derived and *Coleus aromaticus* leaf-derived PF-127 coated TiO_2 NPs inhibited 41% of the A549 cell line [55]. The ROS that accumulated on the surface of the cells may have been induced by the occurrence of capped components of the leaf extract on the PF-127 coated TiO_2 NPs and by the excess electrons that the leaf extract may have provided to the NPs. It elevated oxidative stress, damaged cell membranes, accelerated lipid peroxidation, decreased glutathione levels, and eventually caused cell death [68] (Table 1).

Green Synthesis Approach: The use of A. macrocephala leaf extracts for the synthesis of TiO_2 NPs is a green and

sustainable method. Unlike conventional chemical methods that may involve toxic chemicals and high energy consumption, this approach is environmentally friendly and reduces potential negative impacts on human health and the environment. A. macrocephala is known for its potential bioactive compounds, and these compounds may contribute to the unique properties of the synthesized TiO₂ NPs. The coating of TiO₂ NPs with Pluronic F-127 is an additional step that enhances their stability, dispersibility, and potential for biological applications. This innovative modification can contribute to improved properties and interactions with cells. The thorough characterization techniques applied in this study provide a detailed insight into the physical and chemical properties of the synthesized NPs. This ensures the accurate assessment of their structure, size, and composition, providing a solid foundation for evaluating their properties. The study extensively evaluates the synthesized TiO2 NPs for their antioxidant, antimicrobial, and anticancer activities. This comprehensive assessment allows for a holistic understanding of the NPs' potential applications and benefits. The evaluation of cytotoxicity against multiple cell lines, including HEp-2, KB, and Vero cells, highlights the selectivity of the synthesized NPs. This information is crucial for determining their potential as anticancer agents while maintaining non-toxicity to normal cells. The study suggests that the PF-127-coated TiO₂ NPs could serve as a platform for nanodrug delivery. This aspect could have far-reaching implications for targeted therapy and controlled drug release. The innovative and environmentally friendly approach, along with the multifunctional assessment, positions these TiO2 NPs as promising candidates for various biomedical applications.

HEp-2 and KB cells show similar trends in response to PF-127 coated TiO₂ NPs, with decreasing viability as

concentrations increase. KB cells tend to have slightly lower cell viability than HEp-2 cells. HEp-2 cells tend to have the highest initial viability but decrease more steeply with the increase in the PF-127 coated TiO2 NPs concentrations compared to the other cell lines. Vero cells (normal cells) exhibit consistent viability, showing a relatively negligible amount of cytotoxicity across concentrations and at each time point compared with both HEp-2 and KB cells. A comparison of the IC50 values of KB cells and HEp-2 cells shows that KB cells consistently exhibit the lowest values, indicating a higher sensitivity to the inhibitory effects of PF-127 coated TiO₂ NPs. There is generally a difference in IC50 values depending on the cell line and the time point. KB cells consistently show the lowest IC50 values, suggesting that they are generally more sensitive to PF-127 coated TiO₂ NPs' inhibitory effects in terms of cell viability reduction. As a result of these IC50 values, we are able to determine the potency of PF-127 coated TiO2 NPs when it comes to inhibiting cell viability for different exposure durations. The decreasing trend in IC50 values over time suggests that the cytotoxicity of PF-127 coated TiO2 NPs becomes more pronounced with longer exposure periods. It should be noted that KB cells consistently showed lower IC50 values than HEp-2 cells across all time points, which indicates that KB cells were more sensitive to the effects of PF-127 coated TiO₂ NPs.

Various techniques were used to synthesize and characterize green PF-127 coated ${\rm TiO_2}$ NPs with *A. macroce-phala* leaf extracts. Their antimicrobial, antioxidant, and anticancer properties have also been investigated. The crystallite size of PF-127 coated ${\rm TiO_2}$ NPs were determined to be 60 nm, and the NPs had a polygonal rutile-type crystalline structure. Green PF-127 coated ${\rm TiO_2}$ NPs demonstrated high antimicrobial efficacy against a variety of pathogens. Furthermore, the NPs demonstrated

Table 1: An overview of the efficiency of TiO₂ NPs compared with previous reports

Plant source	Green synthesis method	Antioxidant activity	Antimicrobial activity	Anticancer activity
Aloe vera and Aloe barbadensis [16]	Plant extract	ROS scavenging	Inhibition of pathogens	Induction of apoptosis
Green tea [69]	Leaf extract	Free radical scavenging	Antibacterial effects	Inhibition of cancer cells
Turmeric [70]	Rhizome extract	Antioxidant properties	Antimicrobial potential	Growth inhibition
Neem [71]	Leaf extract	Scavenging of ROS	Broad-spectrum activity	Apoptosis induction
Mexican mint [72]	Leaf extract	ROS neutralization	Antimicrobial effects	Cytotoxicity
Basil [73]	Leaf extract	Antioxidant potential	Inhibition of microorganisms	Cell cycle arrest
Common guava [74]	Leaf extract	ROS quenching	Antibacterial activity	Anti-proliferative effect
Lemon [17,24]	Fruit extract	Free radical scavenging	Antimicrobial properties	Apoptosis induction
Pomegranate [75]	Peel extract	Antioxidant effects	Inhibition of pathogens	Suppression of growth
Ashwagandha [76]	Leaf extract	ROS scavenging	Antimicrobial activity	Antiproliferative action

remarkable antioxidant activity, which increased concentration-dependently. The NPs demonstrated significant cytotoxicity against HEp-2 and KB cell lines, but not against Vero cell lines, indicating their cytotoxic potential against cancer cells. Therefore, PF-127 coated TiO₂ NPs demonstrate remarkable salutary properties to be utilized as a potential antibacterial and anticancer candidate. As a result, further research will focus on utilizing the newly synthesized PF-127 coated TiO₂ NPs for effective design of nanodrug delivery platforms.

5 Conclusion

In conclusion, the PF-127 coated TiO₂ NPs derived from A. macrocephala leaf extracts possess a diverse array of salutary properties. Their antimicrobial, antioxidant, and selective anticancer effects make them promising candidates for applications in antibacterial and anticancer strategies. The synthesized NPs exhibited an average crystallite size of 60 nm and a distinct polygonal rutile-type crystalline structure, confirming their successful formation. Notably, the PF-127 coated TiO₂ NPs displayed heightened antimicrobial efficacy against a diverse range of pathogens, suggesting their potential as potent antibacterial agents. The NPs also demonstrated impressive antioxidant activity, with their efficacy increasing proportionally with concentration. This attribute highlights their potential application as effective antioxidants, holding promise for various health-related applications. A significant finding was the NPs' remarkable cytotoxic effect on cancer cell lines HEp-2 and KB. This selective cytotoxicity underscores their potential as candidates for anticancer therapies, as they effectively target cancer cells while sparing healthy cells from harm. Importantly, the NPs exhibited a non-toxic nature towards Vero cells, indicating their safety profile in relation to healthy cells. This selectivity enhances their attractiveness as potential candidates for cancer treatments with reduced side effects. The next step in the research will involve harnessing the unique properties of these NPs for the development of innovative nanodrug delivery platforms, thereby potentially revolutionizing targeted therapeutic interventions in the field of medicine.

Acknowledgments: It is with gratitude that the author acknowledges the Department of Biochemistry, Faculty of Medicine, Umm Al-Qura University, Makkah, Saudi Arabia for their valuable support and guidance during the research.

Funding information: No research funding was provided.

Author contributions: Riyad A. Almaimani: writing – original draft, writing – review and editing, methodology, formal analysis; visualization, and project administration.

Conflict of interest: Author states no conflict of interest.

Data availability statement: The datasets generated during and/or analysed during the current study are available from the corresponding author on reasonable request.

References

- [1] Santos CS, Gabriel B, Blanchy M, Menes O, García D, Blanco M, et al. Industrial applications of nanoparticles – a prospective overview. Mater Today Proc. 2015;2(1):456–65. doi: 10.13140/2.1. 5100.6726.
- [2] Jahan I, Erci F, Isildak I. Microwave-assisted green synthesis of noncytotoxic silver nanoparticles using the aqueous extract of *Rosa* santana (rose) petals and their antimicrobial activity. Anal Lett. 2019;52(12):1860–73. doi: 10.1080/00032719.2019.1572179.
- [3] Alavi M, Karimi N. Characterization, antibacterial, total antioxidant, scavenging, reducing power and ion chelating activities of green synthesized silver, copper and titanium dioxide nanoparticles using Artemisia haussknechtii leaf extract. Artif Cells Nanomed Biotechnol. 2018;46(8):2066–81. doi: 10.1080/21691401.2017.1408121.
- [4] Bui VK, Tran VV, Moon JY, Park D, Lee YC. Titanium dioxide microscale and macroscale structures: A mini-review. Nanomaterials. 2020;10(6):1190. doi: 10.3390/nano10061190.
- [5] Ziental D, Czarczynska-Goslinska B, Mlynarczyk DT, Glowacka-Sobotta A, Stanisz B, Goslinski T, et al. Titanium dioxide nanoparticles: prospects and applications in medicine. Nanomaterials. 2020;10(2):387. doi: 10.3390/nano10020387.
- [6] Santana I, Wu H, Hu P, Giraldo JP. Targeted delivery of nanomaterials with chemical cargoes in plants enabled by a biorecognition motif. Nat Commun. 2020;11(1):2045. doi: 10.1038/s41467-020-15731-w.
- [7] Irshad MA, Nawaz R, ur Rehman MZ, Imran M, Ahmad J, Ahmad S, et al. Synthesis and characterization of titanium dioxide nanoparticles by chemical and green methods and their antifungal activities against wheat rust. Chemosphere. 2020;258:127352. doi: 10.1016/j.chemosphere.2020.127352.
- [8] Muhd Julkapli N, Bagheri S, Bee Abd Hamid S. Recent advances in heterogeneous photocatalytic decolorization of synthetic dyes. Sci World J. 2014;2014:692307. doi: 10.1155/2014/692307.
- [9] Irshad MA, Nawaz R, ur Rehman MZ, Adrees M, Rizwan M, Ali S, et al. Synthesis, characterization and advanced sustainable applications of titanium dioxide nanoparticles: A review. Ecotoxicol Environ Saf. 2021;212:111978. doi: 10.1016/j.ecoenv.2021.111978.
- [10] Kim TY, Cha SH, Cho S, Park Y. Tannic acid-mediated green synthesis of antibacterial silver nanoparticles. Arch Pharmacal Res. 2016;39:465–73. doi: 10.1007/s12272-016-0718-8.
- [11] Subhapriya S, Gomathipriya P. Green synthesis of titanium dioxide (TiO₂) nanoparticles by *Trigonella foenum-graecum* extract and its

DE GRUYTER

- antimicrobial properties. Microb Pathog. 2018 Mar;116:215–20. doi: 10.1016/j.micpath.2018.01.027. Epub 2018 Jan 31 PMID: 29366863.
- [12] Saratale RG, Karuppusamy I, Saratale GD, Pugazhendhi A, Kumar G, Park Y, et al. A comprehensive review on green nanomaterials using biological systems: Recent perception and their future applications. Colloids Surf B: Biointerfaces. 2018;170:20–35. doi: 10.1016/j.colsurfb.2018.05.045.
- [13] Chahardoli A, Karimi N, Sadeghi F, Fattahi A. Green approach for synthesis of gold nanoparticles from *Nigella arvensis* leaf extract and evaluation of their antibacterial, antioxidant, cytotoxicity and catalytic activities. Artif Cells, Nanomed Biotechnol. 2018;46(3):579–88. doi: 10.1080/21691401.2017.1332634.
- [14] Hossain A, Abdallah Y, Ali MA, Masum MM, Li B, Sun G, et al. Lemon-fruit-based green synthesis of zinc oxide nanoparticles and titanium dioxide nanoparticles against soft rot bacterial pathogen *Dickeya dadantii*. Biomolecules. 2019;9(12):863. doi: 10.3390/ biom9120863.
- [15] Verma V, Al-Dossari M, Singh J, Rawat M, Kordy MGM, Shaban M. A Review on Green Synthesis of TiO₂ NPs: Photocatalysis and Antimicrobial Applications. Polym (Basel). 2022 Apr;14(7):1444. doi: 10.3390/polym14071444. PMID: 35406317. PMCID: PMC9002645.
- [16] Rajkumari J, Magdalane CM, Siddhardha B, Madhavan J, Ramalingam G, Al-Dhabi NA, et al. Synthesis of titanium oxide nanoparticles using *Aloe barbadensis* mill and evaluation of its antibiofilm potential against *Pseudomonas aeruginosa* PAO1. J Photochem Photobiol B. 2019 Dec;201:111667. doi: 10.1016/j. iphotobiol.2019.111667. Epub 2019 Oct 28 PMID: 31683167.
- [17] Ouerghi O, Geesi MH, Riadi Y, Ibnouf EO. Limon-citrus extract as a capping/reducing agent for the synthesis of titanium dioxide nanoparticles: Characterization and antibacterial activity. Green Chem Lett Rev. 2022;15(3):483–90. doi: 10.1080/17518253.2022. 2094205.
- [18] Öztürk UŞ, Çitak A. Synthesis of titanium dioxide nanoparticles with renewable resources and their applications: Review. Turk J Chem. 2022 May;46(5):1345–57. doi: 10.55730/1300-0527.3443. PMID: 37529727. PMCID: PMC10390207.
- [19] Ahn EY, Shin SW, Kim K, Park Y. Facile green synthesis of titanium dioxide nanoparticles by upcycling mangosteen (*Garcinia mangos-tana*) pericarp extract. Nanoscale Res Lett. 2022;17:40. doi: 10.1186/s11671-022-03678-4.
- [20] Velázquez-Hernández AM, García-Rivas JL, Martínez-Gallegos S, González-Juárez JC, Schabes-Retchkiman P, Albiter V. Phytosynthesis of TiO₂ Nanoparticles Using *E. crassipes* Leaf Extracts, Their Photocatalytic Evaluation and Microbicide Effect. Int J Photoenergy. 2022;2022:5177859, 7 pages. doi: 10.1155/2022/ 5177859.
- [21] Dobrucka R. Synthesis of titanium dioxide nanoparticles using *Echinacea purpurea* herba. Iran J Pharm Res. 2017 Spring;16(2):756–62. PMID: 28979329. PMCID: PMC5603885.
- [22] Sethy NK, Arif Z, Mishra PK, Kumar P. Green synthesis of TiO₂ nanoparticles from *Syzygium cumini* extract for photo-catalytic removal of lead (Pb) in explosive industrial wastewater. Green Process Synth. 2020;9(1):171–81. doi: 10.1515/qps-2020-0018.
- [23] Saka A, Shifera Y, Jule LT, Badassa B, Nagaprasad N, Shanmugam R, et al. Biosynthesis of TiO_2 nanoparticles by *Caricaceae* (Papaya) shell extracts for antifungal application. Sci Rep. 2022;12:15960. doi: 10.1038/s41598-022-19440-w.
- [24] Olana MH, Sabir FK, Bekele ET, Gonfa BA. *Citrus sinensis* and *Musa acuminata* Peel Waste Extract Mediated Synthesis of TiO₂/rGO nanocomposites for photocatalytic degradation of methylene blue

- under visible light irradiation. Bioinorg Chem Appl. 2022;2022:5978707, 20 pages. doi: 10.1155/2022/5978707.
- [25] Shaarani S, Hamid SS, Kaus NH. The Influence of pluronic F68 and F127 nanocarrier on physicochemical properties, in vitro release, and antiproliferative activity of thymoquinone drug. Pharmacognosy Res. 2017;9(1):12. doi: 10.4103/0974-8490.199774.
- [26] Manaspon C, Viravaidya-Pasuwat K, Pimpha N. Preparation of folate-conjugated pluronic F127/chitosan core-shell nanoparticles encapsulating doxorubicin for breast cancer treatment. J Nanomaterials. 2012;2012:22. doi: 10.1155/2012/593878.
- [27] Wang X, Peng Y, Tan H, Li M, Li W. Curcumin nanocrystallites are an ideal nanoplatform for cancer chemotherapy. Front Nanosci Nanotech. 2019;5:1–4. doi: 10.15761/FNN.1000186.
- [28] Vu-Quang H, Vinding MS, Nielsen T, Ullisch MG, Nielsen NC, Nguyen DT, et al. Pluronic F127-folate coated super paramagenic iron oxide nanoparticles as contrast agent for cancer diagnosis in magnetic resonance imaging. Polymers. 2019;11(4):743. doi: 10. 3390/polym11040743.
- [29] Domínguez-Delgado CL, Fuentes-Prado E, Escobar-Chávez JJ, Vidal-Romero G, Rodríguez-Cruz IM, Díaz-Torres R. Chitosan and pluronic[®] F-127: Pharmaceutical applications. In Encyclopedia of biomedical polymers and polymeric biomaterials. New York: Taylor and Francis; 2016. pp. 1513–35.
- [30] Le AQH, Nguyen NNT, Tran HD, Nguyen V-H, Tran L-H. A TiO₂@MWCNTs nanocomposite photoanode for solar-driven water splitting. Beilstein J Nanotechnol. 2022;13:1520–30. doi: 10. 3762/bjnano.13.125.
- [31] Rajaraman TS, Gandhi VG, Nguyen VH, Parikh SP. Aluminium foilassisted NaBH₄ reduced TiO₂ with surface defects for photocatalytic degradation of toxic fuchsin basic dye. Appl Nanosci. 2023;13:3925–44. doi: 10.1007/s13204-022-02628-x.
- [32] Cuong HN, Pansambal S, Ghotekar S, Oza R, Thanh Hai NT, Viet NM, et al. New frontiers in the plant extract mediated biosynthesis of copper oxide (CuO) nanoparticles and their potential applications: A review. Environ Res. 2022 Jan;203:111858. doi: 10.1016/j.envres. 2021.111858. Epub 2021 Aug 10 PMID: 34389352.
- [33] Ghotekar S, Pansambal S, Bilal M, Pingale SS, Oza R. Environmentally friendly synthesis of Cr₂O₃ nanoparticles: Characterization, applications and future perspective a review. Case Stud Chem Environ Eng. 2021;3:100089. doi: 10.1016/J.CSCEE. 2021.100089.
- [34] Le SH, Tran MH, Lee JS, Ngo QM, Woo MH, Min BS. Inflammatory inhibitory activity of sesquiterpenoids from *Atractylodes macrocephala* rhizomes. Chem Pharm Bull. 2016;64(5):507–11. doi: 10.1248/ cpb.c15-00805.
- [35] Ji GQ, Chen RQ, Wang L. Anti-inflammatory activity of atractylenolide III through inhibition of nuclear factor-kB and mitogen-activated protein kinase pathways in mouse macrophages. Immunopharmacol Immunotoxicol. 2016;38(2):98–102. doi: 10. 3109/08923973.2015.1122617.
- [36] Song HP, Hou XQ, Li RY, Yu R, Li X, Zhou SN, et al. Atractylenolide I stimulates intestinal epithelial repair through polyamine-mediated Ca²⁺ signaling pathway. Phytomedicine. 2017;28:27–35. doi: 10. 1016/j.phymed.2017.03.001.
- [37] Huang HL, Lin TW, Huang YL, Huang RL. Induction of apoptosis and differentiation by atractylenolide-1 isolated from Atractylodes macrocephala in human leukemia cells. Bioorgan Med Chem Lett. 2016;26(8):1905–9. doi: 10.1016/j.bmcl.2016.03.021.
- [38] Hameed AS, Karthikeyan C, Sasikumar S, Kumar VS, Kumaresan S, Ravi G. Impact of alkaline metal ions Mg²⁺, Ca²⁺, Sr²⁺ and Ba²⁺ on

- the structural, optical, thermal and antibacterial properties of ZnO nanoparticles prepared by the co-precipitation method. J Mater Chem B. 2013;1(43):5950–62. doi: 10.1039/c3tb21068e.
- [39] Hameed AS, Karthikeyan C, Kumar VS, Kumaresan S, Sasikumar S. Effect of Mg²⁺, Ca²⁺, Sr²⁺ and Ba²⁺ metal ions on the antifungal activity of ZnO nanoparticles tested against *Candida albicans*. Mater Sci Eng C. 2015;52:171–7. doi: 10.1016/j.msec.2015.03.030.
- [40] Branca C, Khouzami K, Wanderlingh U, D'Angelo G. Effect of intercalated chitosan/clay nanostructures on concentrated pluronic F127 solution: A FTIR-ATR, DSC and rheological study. J Colloid Interface Sci. 2018;517:221–9. doi: 10.1016/j.jcis.2018.02.004.
- [41] Erdem B, Hunsicker RA, Simmons GW, Sudol ED, Dimonie VL, El-Aasser MS. XPS and FTIR surface characterization of TiO₂ particles used in polymer encapsulation. Langmuir. 2001;17(9):2664–9. doi: 10.1021/la0015213.
- [42] Dhanalakshmi J, Iyyapushpam S, Nishanthi ST, Malligavathy M, Padiyan DP. Investigation of oxygen vacancies in Ce coupled TiO₂ nanocomposites by Raman and PL spectra. Adv Nat Sci Nanosci Nanotechnol. 2017;8(1):015015. doi: 10.1088/2043-6254/aa5984.
- [43] Zheng J, Nagashima K, Parmiter D, de la Cruz J, Patri AK. SEM X-ray microanalysis of nanoparticles present in tissue or cultured cell thin sections. Charact Nanopart Intend drug delivery. 2011;697:93–9. doi: 10.1007/978-1-60327-198-1_9.
- [44] Xu H, Li G, Zhu G, Zhu K, Jin S. Enhanced photocatalytic degradation of rutile/anatase TiO₂ heterojunction nanoflowers. Catal Commun. 2015;62:52–6. doi: 10.1016/j.catcom.2015.01.001.
- [45] Bokuniaeva AO, Vorokh AS. Estimation of particle size using the Debye equation and the Scherrer formula for polyphasic PF-127 coated ${\rm TiO_2}$ powder. J Phys Conf Ser. 2019;1410(1):012057. doi: 10. 1088/1742-6596/1410/1/012057.
- [46] Esfahani RN, Khaghani S, Azizi A, Mortazaeinezhad F, Gomarian M. Facile and eco-friendly synthesis of TiO₂ NPs using extracts of Verbascum thapsus plant: An efficient photocatalyst for reduction of Cr(VI) ions in the aqueous solution. J Iran Chem Soc. 2020;17:205–13. doi: 10.1007/s13738-019-01755-7.
- [47] Pastrana-Martínez LM, Morales-Torres S, Kontos AG, Moustakas NG, Faria JL, Doña-Rodríguez JM, et al. TiO₂, surface modified TiO₂ and graphene oxide-TiO₂ photocatalysts for degradation of water pollutants under near-UV/Vis and visible light. Chem Eng J. 2013;224:17–23. doi: 10.1016/j.cej.2012.11.040.
- [48] Ambika S, Sundrarajan M. [EMIM] BF4 ionic liquid-mediated synthesis of TiO₂ nanoparticles using *Vitex negundo Linn* extract and its antibacterial activity. J Mol Liq. 2016;221:986–92. doi: 10.1016/j. molliq.2016.06.079.
- [49] Reshchikov MA. Measurement and analysis of photoluminescence in GaN. J Appl Phys. 2021;129(12):121101. doi: 10.1063/5.0041608.
- [50] Vijayalakshmi R, Rajendran V. Synthesis and characterization of nano-TiO₂ via different methods. Arch Appl Sci Res. 2012;4(2):1183–90.
- [51] Singh N, Saha P, Rajkumar K, Abraham J. Biosynthesis of silver and selenium nanoparticles by *Bacillus* sp. JAPSK2 and evaluation of antimicrobial activity. Der Pharm Lett. 2014;6(6):175–81.
- [52] Armelao L, Barreca D, Bottaro G, Gasparotto A, Maccato C, Maragno C, et al. Photocatalytic and antibacterial activity of TiO_2 and Au/TiO_2 nanosystems. Nanotechnology. 2007;18(37):375709. doi: 10.1088/0957-4484/18/37/375709.
- [53] Ma HY, Zhao L, Guo LH, Zhang H, Chen FJ, Yu WC. Roles of reactive oxygen species (ROS) in the photocatalytic degradation of pentachlorophenol and its main toxic intermediates by TiO₂/UV. J Hazard Mater. 2019;369:719–26. doi: 10.1016/j.jhazmat.2019.02.080.

- [54] Rajakumar G, Rahuman AA, Roopan SM, Khanna VG, Elango G, Kamaraj C, et al. Fungus-mediated biosynthesis and characterization of TiO₂ nanoparticles and their activity against pathogenic bacteria. Spectrochim Acta Part A: Mol Biomol Spectrosc. 2012;91:23–9. doi: 10.1016/j.saa.2012.01.011.
- [55] Amanulla AM, Sundaram RJ. Green synthesis of TiO₂ nanoparticles using orange peel extract for antibacterial, cytotoxicity and humidity sensor applications. Mater Today Proc. 2019;8:323–31. doi: 10.1016/j.matpr.2019.02.118.
- [56] Bekele ET, Gonfa BA, Zelekew OA, Belay HH, Sabir FK. Synthesis of titanium oxide nanoparticles using root extract of *Kniphofia foliosa* as a template, characterization, and its application on drug resistance bacteria. J Nanomaterials. 2020;2020:1–10. doi: 10.1155/2020/ 2817037.
- [57] Zhang WM, Hu JS, Guo YG, Zheng SF, Zhong LS, Song WG, et al. Tinnanoparticles encapsulated in elastic hollow carbon spheres for high-performance anode material in lithium-ion batteries. Adv Mater. 2008;20(6):1160–5. doi: 10.1002/adma.200701364.
- [58] Kumari MM, Philip D. Synthesis of biogenic SnO₂ nanoparticles and evaluation of thermal, rheological, antibacterial and antioxidant activities. Powder Technol. 2015;270:312–9. doi: 10.1016/j.powtec. 2014.10.034.
- [59] Helmy ET, Abouellef EM, Soliman UA, Pan JH. Novel green synthesis of S-doped TiO₂ nanoparticles using *Malva parviflora* plant extract and their photocatalytic, antimicrobial and antioxidant activities under sunlight illumination. Chemosphere. 2021;271:129524. doi: 10.1016/j.chemosphere.2020.129524.
- [60] Arfin S, Jha NK, Jha SK, Kesari KK, Ruokolainen J, Roychoudhury S, et al. Oxidative stress in cancer cell metabolism. Antioxidants. 2021;10(5):642. doi: 10.3390/antiox10050642.
- [61] Cheng Z, Li M, Dey R, Chen Y. Nanomaterials for cancer therapy: Current progress and perspectives. J Hematol Oncol. 2021;14:85. doi: 10.1186/s13045-021-01096-0.
- [62] Yousefi Rizi HA, Hoon Shin D, Yousefi Rizi S. Polymeric nanoparticles in cancer chemotherapy: A narrative review. Iran J Public Health. 2022 Feb;51(2):226–39. doi: 10.18502/ijph.v51i2.8677. PMID: 35866132. PMCID: PMC9273492.
- [63] Sangour MH, Ali IM, Atwan ZW, Al Ali AA. Effect of Ag nanoparticles on viability of MCF-7 and Vero cell lines and gene expression of apoptotic genes. Egypt J Med Hum Genet. 2021;22(1):9. doi: 10.1186/ s43042-020-00120-1.
- [64] Alzahrani B, Elderdery AY, Alzerwi NAN, Alsrhani A, Alsultan A, Rayzah M, et al. Pluronic-F-127-passivated SnO₂ nanoparticles derived by using *Polygonum cuspidatum* root extract: synthesis, characterization, and anticancer properties. Plants (Basel). 2023 Apr;12(9):1760. doi: 10.3390/plants12091760. PMID: 37176818. PMCID: PMC10181209.
- [65] Alsaiari NS, Alzahrani FM, Amari A, Osman H, Harharah HN, Elboughdiri N, et al. Plant and microbial approaches as green methods for the synthesis of nanomaterials: Synthesis, applications, and future perspectives. Molecules. 2023 Jan;28(1):463. doi: 10.3390/molecules28010463. PMID: 36615655. PMCID: PMC9823860.
- [66] Gebreslassie YT, Gebretnsae HG. Green and cost-effective synthesis of tin oxide nanoparticles: A review on the synthesis methodologies, mechanism of formation, and their potential applications. Nanoscale Res Lett. 2021 May;16(1):97. doi: 10.1186/s11671-021-03555-6. PMID: 34047873. PMCID: PMC8163898.
- [67] De Souza MVF, Shinobu-Mesquita CS, Meirelles LEF, Mari NL, César GB, Gonçalves RS, et al. Effects of hypericin encapsulated on

- Pluronic F127 photodynamic therapy against triple negative breast cancer. Asian Pac J Cancer Prev. 2022 May;23(5):1741-51. doi: 10. 31557/APJCP.2022.23.5.1741. PMID: 35633560. PMCID: PMC9587883.
- [68] Narayanan M, Vigneshwari P, Natarajan D, Kandasamy S, Alsehli M, Elfasakhany A, et al. Synthesis and characterization of TiO2 NPs by aqueous leaf extract of Coleus aromaticus and assess their antibacterial, larvicidal, and anticancer potential. Environ Res. 2021;200:111335. doi: 10.1016/j.envres.2021.111335.
- [69] Selvakumari JC, Ahila M, Malligavathy M, Padiyan DP. Structural, morphological, and optical properties of tin(IV) oxide nanoparticles synthesized using Camellia sinensis extract: A green approach. Int J Min Metall Mater. 2017;24(9):1043-51. doi: 10.1007/s12613-017-1494-2.
- [70] Abdul Jalill RD, Nuaman RS, Abd AN. Biological synthesis of Titanium Dioxide nanoparticles by Curcuma longa plant extract and study its biological properties. World Sci N. 2016;49:204-22.
- [71] Thakur BK, Kumar A, Kumar D. Green synthesis of titanium dioxide nanoparticles using Azadirachta indica leaf extract and evaluation of their antibacterial activity. South Afr J Botany. 2019;124:223-27. doi: 10.1016/J.SAJB.2019.05.024.
- [72] Narayanan M, Vigneshwari P, Natarajan D, Kandasamy S, Alsehli M, Elfasakhany A, et al. Synthesis and characterization of TiO2 NPs by aqueous leaf extract of Coleus aromaticus and assess their anti-

- bacterial, larvicidal, and anticancer potential. Environ Res. 2021 Sep;200:111335. doi: 10.1016/j.envres.2021.111335. Epub 2021 May 27 PMID: 34051200.
- Ahmad MZ, Alasiri AS, Ahmad J, Alqahtani AA, Abdullah MM, Abdel-Wahab BA, et al. Green Synthesis of titanium dioxide nanoparticles using Ocimum sanctum leaf extract: in vitro characterization and its healing efficacy in diabetic wounds. Molecules. 2022;27(22):7712. doi: 10.3390/molecules27227712.
- [74] Santhoshkumar T, Rahuman AA, Jayaseelan C, Rajakumar G, Marimuthu S, Kirthi AV, et al. Green synthesis of titanium dioxide nanoparticles using Psidium quajava extract and its antibacterial and antioxidant properties. Asian Pac J Trop Med. 2014 Dec;7(12):968-76. doi: 10.1016/S1995-7645(14)60171-1. PMID: 25479626.
- [75] Abu-Dalo M, Jaradat A, Albiss BA, Al-Rawashdeh NAF. Green synthesis of TiO₂ NPs/pristine pomegranate peel extract nanocomposite and its antimicrobial activity for water disinfection. J Environ Chem Eng. 2019;7(5):13.
- Maheswari P, Harish S, Navaneethan M, Muthamizhchelvan C, Ponnusamy S, Hayakawa Y. Bio-modified TiO₂ nanoparticles with Withania somnifera, Eclipta prostrata and Glycyrrhiza glabra for anticancer and antibacterial applications. Mater Sci Eng C Mater Biol Appl. 2020 Mar;108:110457. doi: 10.1016/j.msec.2019.110457. Epub 2019 Nov 20 PMID: 31924033.